Preparation, Alignment, and Optical Properties of Soluble Polyphenylacetylene-Wrapped Carbon Nanotubes

Ben Zhong Tang* and Hongyao Xu

Department of Chemistry, Hong Kong University of Science & Technology Clear Water Bay, Kowloon, Hong Kong, China. E-mail: tangbenz@ust.hk.

Carbon nanotubes have been helically wrapped in soluble polyphenylacetylene (PPA) chains by *in situ* polymerization of phenylacetylene in the presence of the nanotubes. The PPAs containing thickly-wrapped short nanotubes (NT/PPAs) are soluble in common organic solvents. Shearing the NT-PPA solutions readily aligns the nanotubes along the shear direction. The NT-PPA solutions limit intense optical pulses and the saturation fluence is tunable by varying the nanotube contents.

The discovery of carbon nanotubes and the prospect of developing carbon-based nanomaterials and technologies excited worldwide interest among researchers (*1*). Thanks to the enthusiastic research efforts of scientists, the nanotubes have quickly proven to possess exotic properties such as high mechanical strength and flexibility (*2*) and diameter- and chirality-dependent electrical conductivity (*3*). The intractability of carbon nanotubes, however, poses an obstacle to the further development in nanotube science and significantly limits the scope of their practical applications. No suitable solvents for the nanotubes have been found, and because of the wet nature of chemistry, this has largely blocked chemists' entry to the area of nanotube research. Solubilization of the nanotubes will not only open up new avenues in nanotube research but also endow the nanotubes with processibility. The nanotubes are known as "quantum wires" (*1*) and polyacetylenes are prototypical "synthetic metals" (*4*). Wrapping the nanotubes with soluble polyacetylene chains may generate novel nanomaterials with intriguingly novel electronic, optical, and magnetic properties, and the ability to orient the polyacetylene chains by external forces (*4, 5*) may allow alignment of the nanotubes by macroscopic means such as mechanical perturbations. In this work, we chose PPA, a soluble photoconductive polyacetylene (*6*), as a model polymer. We describe here a simple method for preparing soluble PPA-wrapped nanotubes (NT-PPA). We demonstrate that the nanotubes in the NT-PPA solutions can be easily aligned by mechanical shear and that the NT-PPA solutions effectively limit intense optical pulses.

During our research program on the development of fullerene-containing optical materials (*7*), we have found that C_{60} can copolymerize with alkynes such as phenylacetylene (*8*). Noting that the nanotubes are conceptually the cylinders of curled graphene sheets capped by fullerene hemispheres, we conducted a polymerization of phenylacetylene catalyzed by WCl_6–Ph_4Sn in the presence of the nanotubes (*9*). The polymer product isolated from the polymerization reaction was characterized by scanning electron microscope (SEM), which shows numerous short tubules with lengths of a few hundred nanometers (Fig. 1A). Such tubular images are not observed in the SEM micrograph of the pure PPA obtained from the control experiment, suggesting that the nanotubes are compounded with PPA *in situ* during the polymerization reaction (Eq. 1). At high magnification, some tubules are found to be linked up, probably by the PPA chains. The thin string marked by letter P in Fig. 1B looks like a stretched PPA "rope" with its two ends attaching to two interconnected nanotubes. Closer inspection of the micrograph, especially in those regions marked by the arrows, reveals that the tubules are surrounded by faint veils, intimating that the nanotubes are bundled or wrapped up by the PPA chains. At some spots, tree-like structures are imaged (Fig. 1C), in which the "trunks" and "branches" of the nanotubes are in all probability sheathed by the "bark" of the PPA chains.

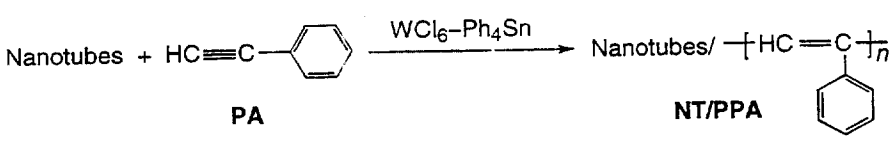

(1)

Table 1. Synthesis and solubility of NT-PPAs; the polymerization reactions were carried out under nitrogen at room temperature in toluene (5 mL) for 24 hours with a phenylacetylene concentration of 0.9 M, and the polymer products were purified by repeated precipitation of their toluene and THF solutions into methanol and hexane.

no.	nanotube (mg)	catalyst[a]	polymer yield (weight %)	$M_w/10^{3}$[b] (g mol^{-1})	PDI[b]	nanotube content[c] (weight %)	solubility[d] THF	toluene	$CHCl_3$	dioxane
1	100	WCl_6–Ph_4Sn	45.3	172	27	6.0	√	√	√	√
2	28	WCl_6–Ph_4Sn	66.8	93	11	1.9	√	√	√	√
3	102	$[Rh(nbd)Cl]_2$	3.4							
4	20	$[Rh(nbd)Cl]_2$	50.2	137	13	2.2	√	√	√	×

[a] $[WCl_6]_o = [Ph_4Sn]_o = 43$ mM; $\{[Rh(nbd)Cl]_2\}_o = 2$ mM, nbd: norbornadiene. [b] Estimated by SEC calibrated with 12 monodisperse polystyrene standards (Waters). [c] Estimated by TGA (Perkin-Elmer TGA 7) under nitrogen. [d] Code: √, completely soluble; ×, partially soluble.

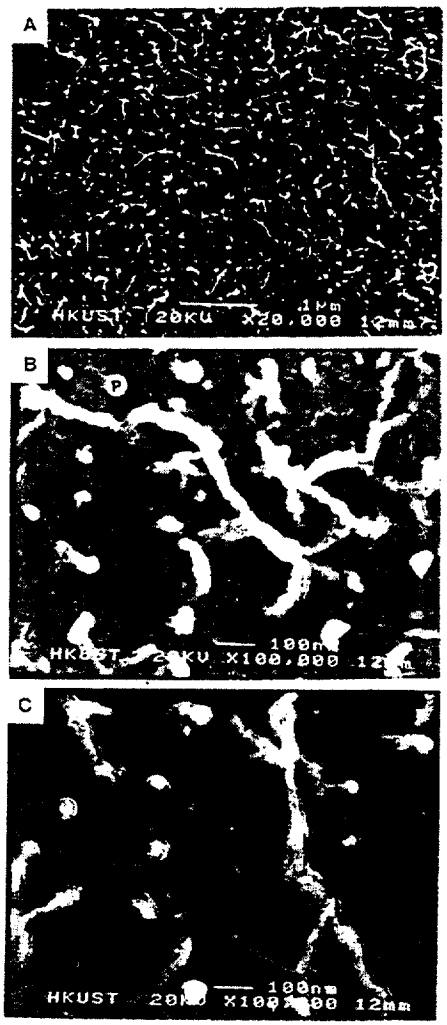

Fig. 1. Nanotubes dispersed in PPA matrix (sample from note 9); micrographs imaged on a JEOL 6300L ultrahigh-resolution scanning electron microscope.

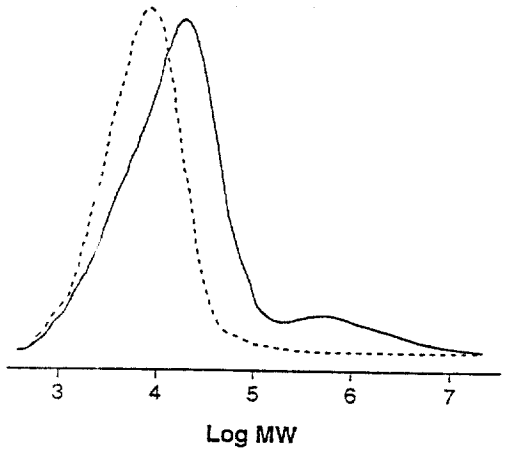

Fig. 2. Size exclusion chromatograms of NT-PPA (solid line; sample from Table 1, no. 1) and PPA (dotted line) recorded on a Waters 510 SEC system with a set of Styragel columns (HT3, HT4, HT6) covering an MW range of 10^2–10^7 g mol^{-1}.

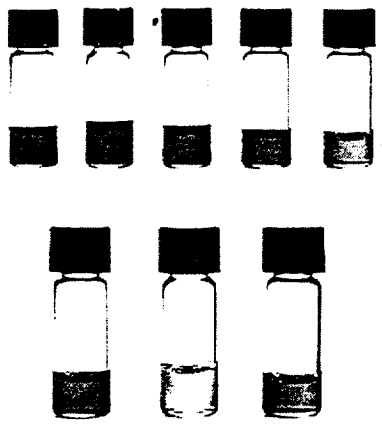

Fig. 3. Homogeneous and transparent solutions of NT-PPA (sample from Table 1, no. 1) in THF with concentrations (c) of (upper panel from left) 19.07, 10.59, 7.15, 5.45, and 3.18 mg mL^{-1}. For comparison, THF solutions of NT-PPA and PPA with similar concentrations are given in the lower panel; c (from left): 5.45 (NT-PPA), 4.00 (PPA), 3.18 (NT-PPA) mg mL^{-1}.

Size exclusion chromatography (SEC) analysis of the NT-PPA gives a bimodal curve, with one large peak in the "normal" molecular weight (MW) region and another small peak in the very high MW region (Fig. 2). Since the high MW peak is not observed in the chromatogram of the control PPA, it should be from the nanotubes compounded with PPA. Because of the contribution of the nanotubes, the polystyrene-calibrated weight-average molecular weight (M_w) of the NT-PPA is very high (172 000 g mol^{-1}) and its polydispersity index (PDI) is extremely broad (27; Table 1, no. 1). It is known that the nanotubes are thermally very stable and do not lose any weight below *ca.* 680°C even in air (*10*); on the other hand, the PPA, stable at room temperature notwithstanding, rapidly loses its weight from *ca.* 200°C (*11*). We thus employed thermogravimetric analysis (TGA) to evaluate the nanotube content of the NT-PPA by heating the polymer to 600°C under nitrogen. By comparison with the TGA data of the control PPA, it is estimated that the NT-PPA contains 6.0 weight % of the nanotubes.

The parent nanotubes are completely insoluble in THF, even with the aid of prolonged sonication. The NT-PPA, however, readily dissolves in THF, giving macroscopically homogeneous and visually transparent solutions (Fig. 3), although its maximum solubility is only about two-thirds of that of the parent PPA in the same solvent. As shown in the lower panel of Fig. 3, a PPA solution with a concentration of 4.00 mg mL^{-1} is yellow in color, while a NT-PPA solution with a lower concentration (3.18 mg mL^{-1}) is orange-colored. The deepening in color is attributable to the dissolved nanotubes, which possess extensively conjugated π-electrons. The NT-PPA is also soluble in other common organic solvents including toluene, chloroform, and 1,4-dioxane, as summarized in Table 1.

When the amount of the nanotubes in the mixture of the polymerization reaction decreases from 100 mg to 28 mg, the yield of the polymer product increases from 45.3% to 66.8% (Table 1, no. 2). In the absence of the nanotubes, the polymer yield is as high as 92.0%. It is thus clear that the presence of the nanotubes in the polymerization mixture decreases the polymer yield. A similar but more pronounced "nanotube effect" is observed when $[Rh(nbd)Cl]_2$ is used as the polymerization catalyst. The polymerization of phenylacetylene in the presence of a large amount (102 mg) of the nanotubes yields little PPA (3.4%). Decreasing the feed amount of the nanotubes to 20 mg dramatically increases the polymer yield to 50.2%, and the polymerization in the absence of the nanotubes produces PPA in quantitative yield. It is possible that the transition metals and the nanotubes have formed some kind of complexes of low catalytic activity, or that the active centers of the polymerization species have undergone chain transfer reactions to the nanotubes, especially when the growing chains are propagating in the close vicinity of the tubule shells.

From all the polymerization reactions carried out in the presence of the nanotubes, fair amounts of insoluble nanotube particles were recovered. When the recovered particles were washed by THF, an excellent solvent for PPA, the solvent was tinted, implying that a small amount of PPA had been attached to the nanotubes. Because of the accuracy in weighing and the ease of handling, we chose the particles recovered from the polymerization with the highest nanotube feed ratio (Table 1, no. 3) for detailed investigation. The recovered nanotube particles were washed thoroughly for prolonged time (*12*), but the amount of the recovered particles (108 mg) was still more than that (102 mg) of the nanotubes initially used in the feed mixture, indicating that the PPA chains had stuck indelibly to the nanotubes.

We thus used transmission electron microscope (TEM) to "see" how the polymer chains are attached to the nanotubes. As can be clearly seen from Fig. 4A, the thinner nanotube is helically wrapped by the PPA coils along the latitudes of tubule shells. Although not so clearly imaged, the tip of the nanotube seems also partially covered by the PPA chains. The thicker neighboring nanotube looks naked, indicating that not all the recovered insoluble nanotubes are wrapped by the PPA chains. Similarly, the thinner nanotube in Fig. 4B is coiled by the PPA helices. In this case, however, the attachment of the PPA chains to the tip of the nanotube is clearly imaged. Since the prolonged washing by THF should have cleaned away the polymer chains physically stuck to the tube *tip*, it is thus likely that the PPA chains are chemically bound to the fullerene hemisphere, probably by the polymerization of phenylacetylene with the C_{60} moiety (*8*). At other spots, some tubules are completely wrapped by the PPA chains, with the helices running perpendicular to the long axes of the tubules (Fig. 4C).

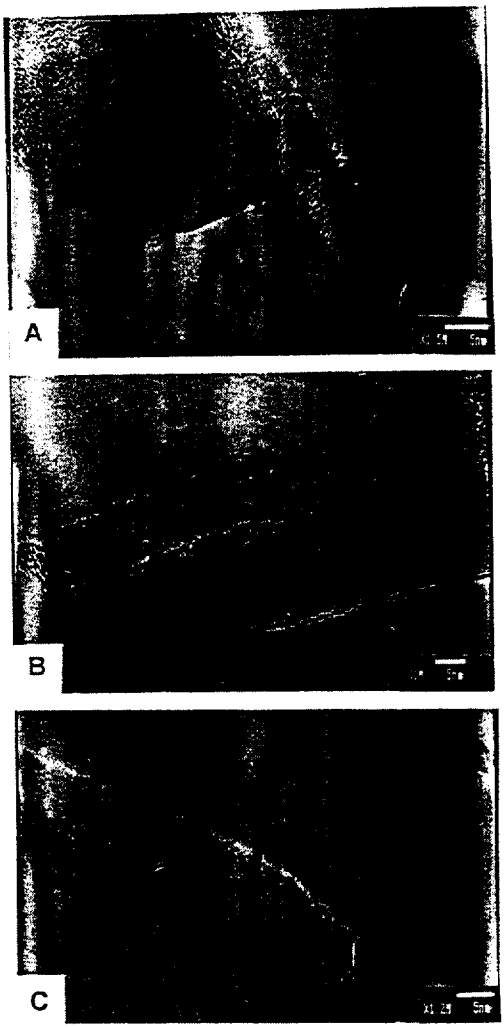

Fig. 4. Wrapping of PPA chains around nanotube shells (sample from note 12); micrographs imaged on a JEOL 2010 transmission electron microscope using an accelerating voltage of 200 kV (scale bar: 5 nm).

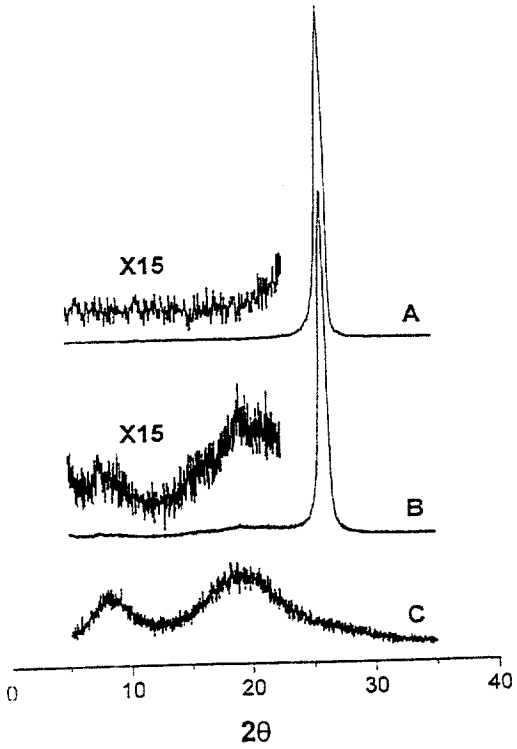

Fig. 5. X-ray diffraction patterns of (A) nanotubes, (B) PPA-wrapped nanotubes (sample from note 12), and (C) PPA; diffratograms recorded on a powder diffractometer (Philips PW1830) with Cu K_α radiation.

To further confirm the identity of the TEM images, we carried out powder X-ray diffraction (XRD) analysis of the recovered insoluble nanotube particles. The XRD pattern of the parent nanotube exhibits an intense (002) Bragg reflection at $2\theta = 26.1°$ (Fig. 5A), corresponding to the intershell spacing (d = 3.4 Å) of the concentric cylinders of graphitic carbon (*13*). The recovered nanotube particles show, in addition to the nanotube reflection, two new weak and broad peaks at lower angles, which, by comparison with the diffractogram shown in Fig. 5C, are clearly the reflection peaks of the PPA chains. The XRD data thus support the correlation of the TEM images; that is, the coils wrapping around the tubule shells and attaching to the tubule tips are the amorphous PPA chains.

To check whether or not PPA chains can be attached to the nanotubes by simple physical blending, a control experiment was conducted, in which the nanotubes and the preformed (pure) PPA were admixed and stirred in toluene for 24 hours. Following the filtration and precipitation procedures detailed in note 9, all the nanotubes were recovered and the color of the PPA solution remained unchanged. The microscopic analyses show neither the PPA chains in the recovered nanotubes nor the tubular entity in the recovered PPA. The nanotubes thus may be wrapped by the propagating species of the PPA chains *in situ* during the polymerization reactions.

Terminal alkynes (RC≡C-H) often form ≡C-H···π hydrogen bonds with molecules or groups that are rich in π-electrons (*14*). Because the nanotubes are full of π-electrons, the phenylacetylene

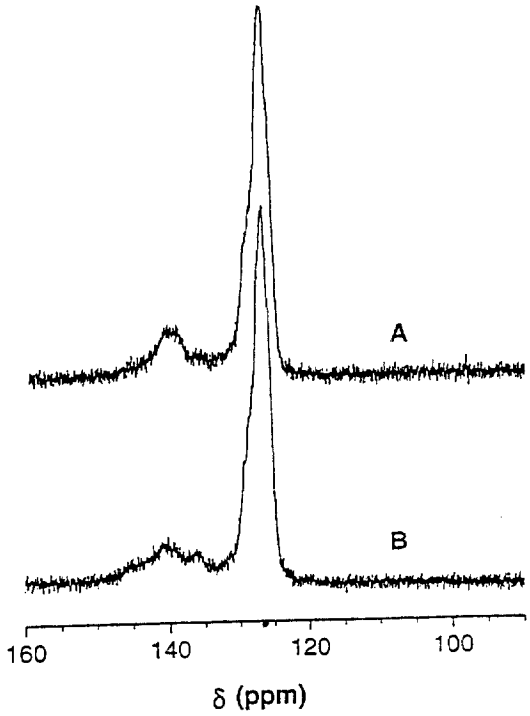

Fig. 6. ^{13}C NMR spectra of (A) NT-PPA (sample from Table 1, no. 1) and (B) PPA recorded on a Bruker ARX300 NMR spectrometer using chloroform-*d* as solvent and tetramethylsilane as internal reference.

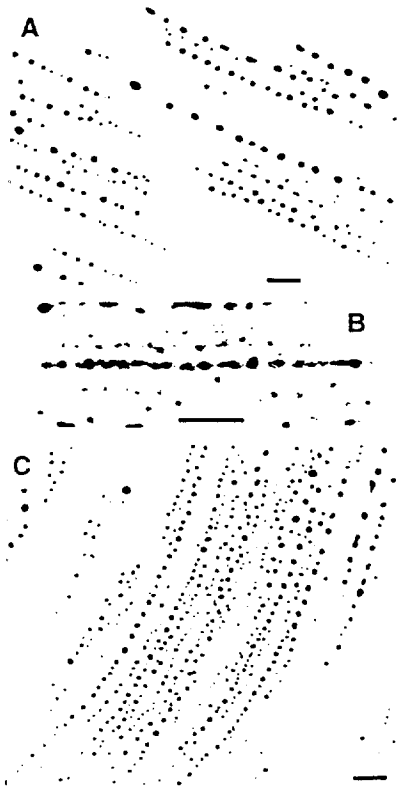

Fig. 7. Alignment of nanotubes induced by mechanical shear; microphotographs taken on an Olympus BX60 optical microscope (scale bar: 10 μm).

monomers are likely to "wet" the surfaces of the tubule shells through the ≡C-H···π hydrogen bonds, and polymerization of such absorbed monomers would produce the PPA chains wrapping up the nanotubes. Polymerizations of internal alkynes without the acidic acetylene hydrogen such as $CH_3C{\equiv}CPh$ failed to incorporate any nanotubes into the resulting polyacetylenes, further suggesting the important role of the ≡C-H···π hydrogen bonds in the wrapping processes of the nanotubes by the PPA chains. Polyacetylenes containing chiral substituents possess helical conformation (*15*) and complexation of PPA derivatives with chiral molecules are known to induce helix formation (*16*). The nanotubes are cylinders of rolled-up graphene sheets with various chiralities (*3*), and the propagating species of the polymer chains may experience stereochemical interaction with the chiral tubules, thus generating the PPA helices spiraling around the nanotubes. When the short nanotubes are thickly wrapped by the PPA chains, the solvation of the polymer molecules may drag the tubules into the solvent, thus making the nanotubes "soluble". On the other hand, the long tubules unwrapped or thinly wrapped by the PPA chains would remain insoluble in the organic solvents.

The solubility of the short nanotubes wrapped by the PPA chains enables the characterization of their molecular structure by wet spectroscopy and the investigation of their solution properties. The ^{13}C nuclear magnetic resonance (NMR) spectrum of the chloroform solution of the NT/PPA is almost identical to that of the parent PPA, except for that the peak of the NT/PPA at δ *ca.* 140 becomes more intense (Fig. 6). The solid-state NMR spectrum of the parent nanotubes shows a broad peak centered at δ 130 and the acid-functionalized nanotubes absorb at δ *ca.* 145. The increase in the peak intensity at δ *ca.* 140 thus may be attributed to the absorption of the nanotubes wrapped by the PPA chains.

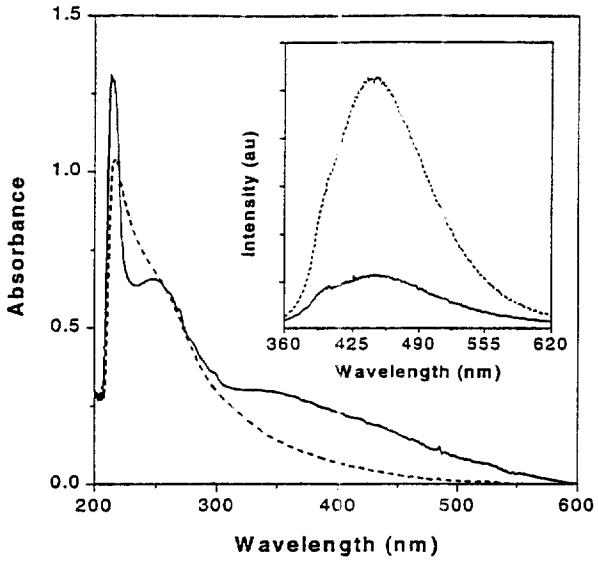

Fig. 8. Electronic absorption and fluorescence emission (inset) spectra of THF solutions of NT-PPA (solid line; sample from Table 1, no. 1) and PPA (dotted line) recorded on a Milton Roy 3000 spectrophotometer and a SLM Aminco JD-490 spectrofluorometer (excited at 350 nm); concentration (mg/mL): 0.01 (absorption), 0.10 (emission).

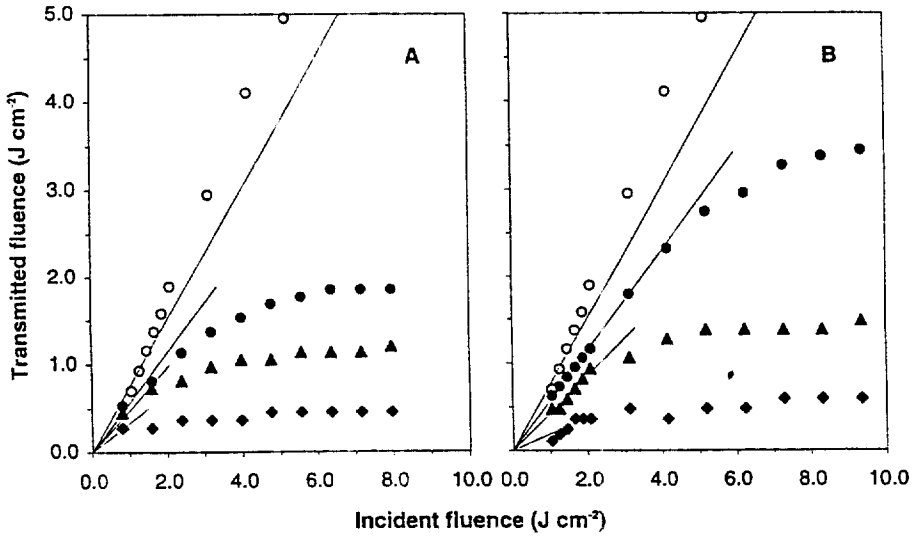

Fig. 9. Optical limiting responses of THF solutions of the NT-PPAs prepared by (A) WCl_6–Ph_4Sn (sample from Table 1, no. 1) and (B) $[Rh(nbd)Cl]_2$ (Table 1, no. 4); concentration (c; mg mL^{-1})/linear transmittance (T; %): (A) 0.4/57 (●), 0.5/48 (▲), 0.6/34 (◆); (B) 1.0/57 (●), 2.0/42 (▲), 3.0/19 (◆). Optical responses of a THF solution of PPA are shown for comparison [c (mg mL^{-1})/T (%): 4.0/75 (○)]. The 8-ns pulses of 532-nm light were generated from a Quanta Ray GCR-3 frequency-doubled Q-switched Nd:YAG laser.

We have recently found that liquid crystalline polyacetylenes can be oriented by external forces (*5*), and it is of interest to know whether the nanotubes in the NT-PPA solutions can be aligned by mechanical shear. When a thin layer of concentrated THF solution of NT-PPA sandwiched between two pieces of glass slides was sheared and then allowed to stand at room temperature for *ca.* 20

minutes, the uniform background of the homogeneous solution was embellished with numerous tiny spots aligning along the shear direction (Fig. 7A), which was not observed in the control experiment using the THF solution of pure PPA. The nanotubes would aggregate as the solvent of the sandwiched solution slowly evaporates, but the surrounding PPA chains would prevent the aggregates from growing bigger, thus resulting in the formation of the tiny micelle-like spots. Careful examination at high magnification during the emerging stage of the aggregates from the homogeneous solution finds the necklace-like textures (Fig. 7B), in which tiny black "pearls" of the nanotube clusters are strung together, probably by the oriented PPA chains. This suggests that the alignment of the nanotube aggregates along the shear direction is assisted, at least in part, by the shear-induced orientation of the stiff polyacetylene chains (*5*). When a curved or bent shear force is applied, the nanotubes align along the curvature of shear direction (Fig. 7C), demonstrating the ease with which the nanotubes may be manipulated and aligned by simple mechanical perturbation.

While the parent PPA weakly absorbs in the visible spectral region, the absorption of the NT-PPA well extends to *ca.* 600 nm, in agreement with its deeper color (Fig. 8). When the PPA is excited at 350 nm, it emits fluorescence with a peak maximum at *ca.* 450 nm. The fluorescence spectral profile of the NT-PPA is similar to that of the PPA, but with much lower quantum yield. The decrease in the fluorescence intensity of the NT-PPA may be caused by absorption, quenching, and scattering of the nanotubes.

Fullerenes and polyacene-based oligomers with graphite-like structures are known to limit intense optical pulses by reverse saturable absorption mechanisms (*17*). The fullerene tips and the graphene sheets of the short carbon nanotubes may undergo nonlinear optical (NLO) absorption processes. Moreover, the cylindrical bodies of the nanotubes, albeit with high length/diameter ratio, may function as light scattering centers. Both the NLO absorption and scattering would make the nanotubes promising candidates for optical limiters (*18*). We thus investigated optical responses of the NT/PPA solutions to laser pulses, employing the similar experimental setup used in our previous studies on the optical limiting properties of fullerene materials (*19*).

When a THF solution of the parent PPA is shot by the 8-ns pulses of 532-nm laser light, the transmitted fluence linearly increases in the low incident-fluence region (Fig. 9). The output starts and continues to deviate from the linear-transmission line from the input of *ca.* 1.7 J cm^{-2}, implying that the intense illumination gradually bleaches the PPA to transparency, probably by the laser-induced photolysis of the polyacetylene chains. The NT-PPA solutions, however, respond to the optical pulses in a strikingly different way. The linear transmittance of a dilute NT-PPA solution (0.4 mg mL^{-1}) is only 57% (Fig. 9A), although its concentration is only a tenth of that (4 mg mL^{-1}) of the parent PPA, probably because of the optical losses caused by the nanotube absorption and scattering. As the incident fluence increases, the NT-PPA solution becomes opaque, instead of transparent, with its transmitted fluence eventually leveling off or saturating at 1.85 J cm^{-2} (saturation fluence). Clearly the nanotubes have endowed the NT-PPA with optical limiting power. The energy-sinking and radical-trapping functions of aromatic rings often prevent polymer molecules from photodegradation (*20*), and the extensively conjugated graphitic aromatic system of the nanotubes may have enhanced the resistance of the PPA chains against the laser irradiation. When the concentration of the NT-PPA solution increases, its saturation fluence decreases. Increasing the concentration to 0.6 mg mL^{-1} readily decreases the saturation fluence to as low as 0.45 J cm^{-2}.

Similarly, the NT-PPA prepared by the $[Rh(nbd)Cl]_2$ catalyst also limits the intense optical pulses (Fig. 9B). A THF solution of the NT-PPA with a concentration of 1.0 mg mL^{-1} exhibits a saturation fluence of 3.44 mg cm^{-2}, which is much higher than those of the THF solutions of the NT-PPA prepared by WCl_6-Ph_4Sn with lower concentrations (*cf.* Fig. 9A). The major difference between the two NT-PPAs is their nanotube content. The NT-PPA with lower nanotube content shows higher saturation fluence, further confirming that the nanotubes are responsible for the optical limiting in the NT-PPA solutions. In this case again, increasing the concentration decreases the saturation fluence. A low saturation fluence of 0.58 J cm^{-2} is achieved when the concentration is increased to 3 mg mL^{-1}.

In summary, in this study, short carbon nanotubes have been solubilized by wrapping them with soluble PPA chains. Solubility is the primary requirement for studying wet chemistry, and this work paves the way for new approaches to nanotube science and will lead to new developments in nanotube chemistry. The helical wrapping of the PPA chains along the latitudes of the carbon nanotubes is of technological interest. One intriguing possibility is the creation of molecular-level electromagnetic devices such as "nanomotors" through molecular engineering endeavor to magnetize the nanotubes by

the electrical field generated by the photoconductive PPA coils. Ready alignment of the nanotubes has been demonstrated and this provides a versatile means for macroscopically manipulating the nanotubes. Furthermore, the NT-PPA solutions have been found to limit the intense optical pulses. Since the control of light intensity is of fundamental importance in optics engineering, the NT-PPA system examined here may find an array of potential applications in optics-related especially laser-based technologies.

REFERENCES AND NOTES

1. M. Endo, S. Iijima, M. S. Dresselhaus, Eds. *Carbon Nanotubes* (Pergamon, Oxford, 1996); T. W. Ebbesen, Ed. *Carbon Nanotubes: Preparation and Properties* (CRC Press, Boca Raton, FL, 1997).
2. M. M. J. Treacy, T. W. Ebbesen, J. M. Gibson, *Nature* **381**, 678 (1996); M. R. Falvo *et al.*, *ibid.* **389**, 582 (1997).
3. J. W. G. Wildoer, L. C. Venema, A. G. Rinzler, R. E. Smalley, C. Dekker, *ibid.* **391**, 59 (1998); T. W. Odom, J.-L. Huang, P. Kim, C. M. Lieber, *ibid.*, p. 62.
4. C. Taliani, Z. V. Vardeny, Y. Maruyama, Eds. *Synthetic Metals for Non-Linear Optics and Electronics* (European Materials Research Society, Amsterdam, 1993); A. Akagi, H. Shirakawa, *Macromol. Symp.* **104**, 137 (1996).
5. B. Z. Tang *et al.*, *Macromolecules* **31**, 2419 (1998); X. Kong, B. Z. Tang, *Chem. Mater.* in press.
6. E. T. Kang, P. Ehrlich, A. P. Bhatt, W. A. Anderson, *ibid.* **17**, 1020 (1984).
7. B. Z. Tang, S. M. Leung, H. Peng, N. T. Yu, K. C. Su, *ibid.* **30**, 2848 (1997); *Adv. Mater.* **8**, 939 (1996).
8. H. Xu, B. Z. Tang, *Abstr. 5th Symp. Chem. PG Res. HK* P-28 (1998).
9. Into a baked 20-mL Schlenk tube under dry nitrogen were added 100 mg of multi-walled nanotubes (from MER), 95 mg of WCl_6, 102 mg of Ph_4Sn, 5 mL of toluene, and 0.55 mL of phenylacetylene (all from Aldrich). The mixture was stirred at room temperature for 24 hours. Toluene (5 mL) was then added to the Schlenk tube and the diluted reaction mixture was filtered by a cotton filter to remove insoluble nanotube particles. The soluble filtrate was added dropwise into 250 mL of methanol with stirring to precipitate the polymeric product. The precipitant was isolated using a Gooch crucible filter and dried in a vacuum oven. The product was redissolved in tetrahydrofuran (THF) and the resulting solution was centrifuged at 2 000 rpm for 16 minutes. The supernatant was added through a cotton filter into hexane. The precipitant was collected and then dried under vacuum at 40°C to a constant weight; yield: 45.3 weight % (Table 1, no. 1).
10. P. M. Ajayan *et al.*, *Nature* **362**, 522 (1993); S. C. Tsang, P. J. F. Harris, M. L. H. Green, *ibid.*, p. 520.
11. T. Masuda, B. Z. Tang, H. Higashimura, H. Yamaoka, *Macromolecules* **18**, 2369 (1985).
12. The insoluble nanotube particles recovered from the reaction no. 3 of Table 1 were repeatedly washed by THF. The solvent was tinged yellowish in the beginning of the washing but became colorless at the end. The particles were further soaked in THF for 20 days but the solvent remained uncolored. The particles separated from the supernatant were washed with fresh THF again and then dried *in vacuo* to a constant weight (108 mg).
13. O. Zhou *et al.*, *Science* **263**, 1744 (1994).
14. H.-C. Weiss, D. Blaser, R. Boese, B. M. Dougham, M. M. Haley, *Chem. Commun.* 1703 (1997); T. Stein, *ibid.* 95 (1995).
15. F. Ciardelli, S. Lanzillo, O. Pieroni, *Macromolecules* **7**, 174 (1974); J. S. Moore, C. B. Gorman, R. H. Grubbs, *J. Am. Chem. Soc.* **113**, 1704 (1991); Q. Sun, B. Z. Tang, *Abstr. 5th Symp. Chem. PG Res. HK* O-54 (1998).
16. E. Yashima, T. Matsushima, Y. Okamoto, *J. Am. Chem. Soc.* **119**, 6345 (1997).
17. L. W. Tutt, A. Kost, *Nature* **356**, 225 (1992); Y. Kojima, *et al. Macromolecules* **28**, 2893 (1995).
18. L. W. Tutt, T. F. Boggess, *Prog. Quant. Electr.* **17**, 299 (1993).
19. B. Z. Tang *et al.*, in *Materials for Optical Limiting II*, R. Sutherland *et al.*, Eds. (MRS, Pittsburgh, PA, 1998), pp. 69-74; B. Z. Tang, *et al. Macromolecules* **31**, 103 (1998).
20. G. Scott, Ed. *Mechanisms of Polymer Degradation and Stabilisation* (Elsevier, London, 1990).

21. This paper was submitted to *Science* on June 20, 1998 (*received June 22, 1998*). This project was in part supported by the Hong Kong Research Grants Council and the HKUST-CAS Nanostructure Materials and Technology Joint Laboratory. We thank Y. Zhang for her help in the SEM and TEM measurements, M. W. Fok for his assistance in the optical limiting experiment, and I. Bytheway for proofreading of the manuscript.